J. Fluid Mech. (1991), *vol.* 224, *pp.* 645–659
Printed in Great Britain

Hydrodynamic forces on a submerged cylinder advancing in water waves of finite depth

By G. X. WU

Department of Mechanical Engineering, University College London, Torrington Place, London WC1E 7JE, UK

(Received 29 May 1990)

The hydrodynamic problem of a submerged horizontal cylinder advancing in regular water waves of finite depth at constant forward speed is analysed by the linearized velocity potential theory. The Green function is first derived. Far-field equations for calculating damping coefficients and exciting forces are obtained. The numerical method used combines a finite-element approximation of the potential in a region surrounding the cylinder with a boundary-integral-equation representation of the outer region. Numerical results for the hydrodynamic forces on submerged circular cylinders and elliptical cylinders are provided.

1. Introduction

The work on the linearized potential problem of a submerged horizontal cylinder advancing in regular water waves at constant forward speed has been hitherto limited to infinite water depth. Grue & Palm (1985) considered a special case of the circular cylinder using the source distribution method. For this particular problem the source distribution over the cylinder surface could be written as the Fourier series. The boundary-integral equation for the source distribution is then transferred to an infinite set of linear equation for the coefficients in the series. A more general case of an elliptical cylinder was solved by Mo & Palm (1987) using a numerical method for the high-order source distribution over the cylinder. The solution of an arbitrary submerged non-lifting cylinder was obtained by Wu & Eatock Taylor (1987) using the coupled finite-element method. The method combines a finite-element representation of the potential in the near field with an integral representation in the far field. It has a particular advantage in that it avoids the calculation of the second-order derivatives of the steady potential.

In this work we shall solve the problem of a submerged cylinder in finite water depth. The water depth is known to have a marked effect on various linearized free-surface flow problems. We shall investigate its effect on the present problem by first deriving the Green function. A summary of the coupled finite-element method then follows. Numerical results are provided for hydrodynamic coefficients and exciting forces. Comparison is made between results obtained from the integration of the pressure over the cylinder surface and far-field equations derived in this paper and excellent agreement is found.

2. Governing equations

We define the right-handed coordinate system $O\text{-}xyz$ so that x points in the direction of forward speed U and z points upwards. The origin of the coordinates is located on the undisturbed free surface. The whole system is moving with the body at the same speed. For a time-periodic incoming wave at a frequency ω_0, the total potential can be written as

$$\Phi = -Ux + U\bar{\phi} + \mathrm{Re}\,[(\eta_0\phi_0 + \eta_1\phi_1 + \eta_3\phi_3 + \eta_5\phi_5 + \eta_7\phi_7)\,e^{i\omega t}], \tag{1}$$

where $\bar{\phi}$ is the steady potential due to unit forward speed; $\phi_j\,(j = 1, 3, 5)$ are the radiation potentials associated with translations in the x- and z-directions and rotation about y respectively; $\eta_j\,(j = 1, 3, 5)$ are corresponding motion amplitudes; ϕ_0 and ϕ_7 are the potentials of the incident and diffracted waves respectively; and $\eta_0 = \eta_7$ is the incoming wave amplitude. The encounter frequency ω is obtained from

$$\omega = \omega_0 \pm k_0 U, \tag{2a}$$

$$k_0 \tanh(k_0 d) = \omega_0^2/g, \tag{2b}$$

where d is the water depth, the $+$ sign corresponds to the incident wave coming from the right-hand side of the cylinder and the $-$ sign corresponds to the wave from the left.

Based on the assumptions of the linearized theory, we have the governing equations for the steady potential

$$\nabla^2\bar{\phi} = \frac{\partial^2\bar{\phi}}{\partial x^2} + \frac{\partial^2\bar{\phi}}{\partial z^2} = 0 \tag{3}$$

in the whole fluid domain;

$$\frac{\partial\bar{\phi}}{\partial n} = n_x \tag{4}$$

on the cylinder surface S_0, where $\boldsymbol{n}$ is the inward normal from the cylinder surface and n_x is the component of $\boldsymbol{n}$ in the x-direction;

$$\mu\bar{\phi}_z + \bar{\phi}_{xx} = 0 \tag{5}$$

on the free surface S_F or $z = 0$, where $\mu = g/U^2$; and

$$\frac{\partial\bar{\phi}}{\partial z} = 0 \tag{6}$$

on the bottom of the fluid. The far-field behaviour of ϕ can be specified as

$$\frac{\partial\bar{\phi}}{\partial x} = 0 \quad \text{as} \quad x \rightarrow +\infty, \tag{7a}$$

$$\frac{\partial\bar{\phi}}{\partial x} = \begin{cases} w(x,z) \text{ if } & Fn = U/(gd)^{\frac{1}{2}} < 1 \\ 0 \quad\text{ if } & Fn = U/(gd)^{\frac{1}{2}} > 1 \end{cases} \quad \text{as} \quad x \rightarrow -\infty, \tag{7b}$$

where $w(x,z)$ corresponds to a wave oscillating with x.

The components of the radiation and diffraction potentials satisfy the following equations (Newman 1978):

$$\nabla^2\phi_j = 0 \tag{8}$$

in the whole fluid domain;

$$\phi_{jz} + (\tau^2/\nu)\,\phi_{jxx} - 2i\tau\phi_{jx} - \nu\phi_j = 0 \tag{9}$$

on the free surface, where $\tau = \omega U/g$ and $\nu = \omega^2/g$;

$$\frac{\partial\phi}{\partial z} = 0 \tag{10}$$

on the bottom of the fluid;

$$\frac{\partial \phi_j}{\partial n} = \mathrm{i}\omega n_j + U m_j \quad (j = 1,3,5), \tag{11a}$$

$$\frac{\partial \phi_7}{\partial n} = -\frac{\partial \phi_0}{\partial n} \tag{11b}$$

on the cylinder surface, with

$$(n_1, n_3, n_5) = (n_x, n_z, z n_x - x n_z) \tag{12a}$$

and

$$(m_1, m_3, m_5) = -\left\{\frac{\partial \bar{\phi}_x}{\partial n}, \frac{\partial \bar{\phi}_z}{\partial n}, \left(\frac{\partial}{\partial n}\right)[z(\bar{\phi}_x - 1) - x\bar{\phi}_z]\right\}. \tag{12b}$$

The radiation condition for $\phi_j\,(j = 1,3,5,7)$ states that a wave travelling in the direction of the forward speed and with its group velocity larger than the forward speed is far in front of the body, and otherwise the waves propagate behind.

3. Green function

The Green function is defined as the potential of a source undergoing the same motions as the cylinder. A brief discussion has been given by Becker (1956). We may write it as

$$G(x,z,\xi,\zeta) = \ln(r/d) + \ln(r_2/d) + H(x,z,\xi,\zeta), \tag{13}$$

where

$$r = [(x-\xi)^2 + (z-\zeta)^2]^{\frac{1}{2}}, \tag{14a}$$

$$r_2 = [(x-\xi)^2 + (z+\zeta+2d)^2]^{\frac{1}{2}}. \tag{14b}$$

The first term is due to a source located at (ξ, ζ) and the second is its mirror image about the bottom of the fluid. The sum of these two terms satisfies the boundary condition on the horizontal bottom $z = -d$. $H(x,z,\xi,\zeta)$ is regular in the whole fluid domain. Since

$$\ln\left(\frac{r}{d}\right) = \int_0^\infty \frac{\mathrm{e}^{-md} - \mathrm{e}^{-m|z-\zeta|}\cos m(x-\xi)}{m}\,\mathrm{d}m, \tag{15a}$$

$$\ln\left(\frac{r_2}{d}\right) = \int_0^\infty \frac{\mathrm{e}^{-md} - \mathrm{e}^{-m(z+\zeta+2d)}\cos(x-\xi)}{m}\,\mathrm{d}m \tag{15b}$$

we may write H in the following form:

$$H = \int_0^\infty \{\cosh m(z+d)\,[A(m)\,\mathrm{e}^{-\mathrm{i}m(x-\xi)} + B(m)\,\mathrm{e}^{\mathrm{i}m(x-\xi)}] + C(m)\}\,\mathrm{d}m, \tag{16}$$

which satisfies the Laplace equation and bottom boundary condition. By imposing the free-surface condition in (9) on G, we obtain

$$A(m) = \frac{-[m\nu + (\tau m)^2 + 2\tau m\nu + \nu^2]}{m\nu[m\tanh(md) - (\tau m)^2/\nu - 2\tau m - \nu]}\,\frac{\mathrm{e}^{-md}\cosh m(\zeta+d)}{\cosh(md)}, \tag{17a}$$

$$B(m) = \frac{-[m\nu + (\tau m)^2 - 2\tau m\nu + \nu^2]}{m\nu[m\tanh(md) - (\tau m)^2/\nu + 2\tau m - \nu]}\,\frac{\mathrm{e}^{-md}\cosh m(\zeta+d)}{\cosh(md)}, \tag{17b}$$

$$C(m) = -2\mathrm{e}^{-md}/m. \tag{17c}$$

It can be seen that $A(m)$ or $B(m)$ are singular when $m\nu \tanh(md) = (\tau m+\nu)^2$ or $m\nu\tanh(md) = (\tau m-\nu)^2$. The latter always has two solutions, k_3 and k_4, with $k_3 > k_4$; but care is needed in the first equation. We may write it as

$$\sigma = Um+\omega = [mg\tanh(md)]^{\frac{1}{2}}, \tag{18}$$

where σ is the frequency in the fixed coordinate system. We plot this equation in figure 1. It is apparent that for a sufficiently large U there is no solution. When U decreases to U_c there will be one solution at which the derivatives of both sides of (18) are identical, or

$$U = C_g = \frac{\sigma}{2m}\left[1+\frac{2md}{\sinh(2md)}\right], \tag{19}$$

where $C_g = \mathrm{d}\sigma/\mathrm{d}m$ is the group velocity in the fixed system. When U further decreases there will be two solutions, k_1 and k_2, with $k_1 > k_2$.

Invoking the radiation condition, we can write the Green function as

$$\begin{aligned}
G = {} & \ln(r/d)+\ln(r_2/d) \\
& +2\int_0^\infty \frac{\mathrm{e}^{-md}}{m}\left\{\frac{\cosh m(\zeta+d)\cosh m(z+d)}{\cosh md}\cos m(x-\xi)-1\right\}\mathrm{d}m \\
& +\mathrm{PV}\int_0^\infty \frac{\nu[1+\tanh(md)]}{(\tau m)^2+2\tau\nu m-m\nu\tanh(md)+\nu^2}\,\frac{\mathrm{e}^{-md}\cosh m(\zeta+d)}{\cosh(md)} \\
& \qquad\qquad \times\cosh m(z+d)\,\mathrm{e}^{-\mathrm{i}m(x-\xi)}\,\mathrm{d}m \\
& +\mathrm{PV}\int_0^\infty \frac{\nu[1+\tanh(md)]}{(\tau m)^2-2\tau\nu m-m\nu\tanh(md)+\nu^2}\,\frac{\mathrm{e}^{-md}\cosh m(\zeta+d)}{\cosh(md)} \\
& \qquad\qquad \times\cosh m(z+d)\,\mathrm{e}^{\mathrm{i}m(x-\xi)}\,\mathrm{d}m \\
& +\pi\mathrm{i}\frac{\nu[1+\tanh(k_1d)]}{2\tau^2k_1+2\tau\nu-\nu\tanh(k_1d)-k_1\nu d\,\mathrm{sech}^2(k_1d)}\,\frac{\mathrm{e}^{-k_1d}\cosh k_1(\zeta+d)}{\cosh(k_1d)} \\
& \qquad\qquad \times\cosh k_1(z+d)\,\mathrm{e}^{-\mathrm{i}k_1(x-\xi)} \\
& -\pi\mathrm{i}\frac{\nu[1+\tanh(k_2d)}{2\tau^2k_2+2\tau\nu-\nu\tanh(k_2d)-k_2\nu d\,\mathrm{sech}^2(k_2d)}\,\frac{\mathrm{e}^{-k_2d}\cosh k_2(\zeta+d)}{\cosh(k_2d)} \\
& \qquad\qquad \times\cosh k_2(z+d)\,\mathrm{e}^{-\mathrm{i}k_2(x-\xi)} \\
& -\pi\mathrm{i}\frac{\nu[1+\tanh(k_3d)]}{2\tau^2k_3-2\tau\nu-\nu\tanh(k_3d)-k_3\nu d\,\mathrm{sech}^2(k_3d)}\,\frac{\mathrm{e}^{-k_3d}\cosh k_3(\zeta+d)}{\cosh(k_3d)} \\
& \qquad\qquad \times\cosh k_3(z+d)\,\mathrm{e}^{\mathrm{i}k_3(x-\xi)} \\
& -\pi\mathrm{i}\frac{\nu[1+\tanh(k_4d)]}{2\tau^2k_4-2\tau\nu-\nu\tanh(k_4d)-k_4\nu d\,\mathrm{sech}^2(k_4d)}\,\frac{\mathrm{e}^{-k_4d}\cosh k_4(\zeta+d)}{\cosh(k_4d)} \\
& \qquad\qquad \times\cosh k_4(z+d)\,\mathrm{e}^{\mathrm{i}k_4(x-\xi)},
\end{aligned} \tag{20}$$

where PV indicates the principal-value integration. In this equation, the k_1 and k_2 waves travel in the direction of the forward speed; but only the k_2 wave has its group velocity larger than the forward speed and therefore is located far in front of the body. When there is no solution from (18) the terms involving k_1 and k_2 should be deleted from (20).

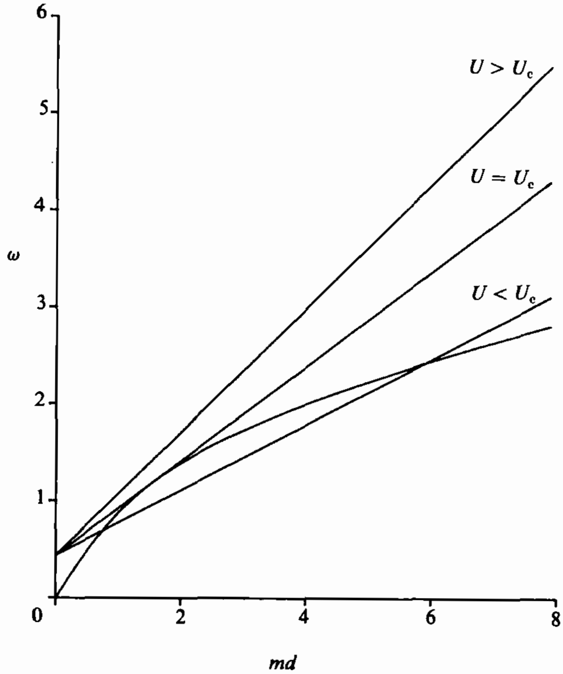

FIGURE 1. Graphical solution of equation (18).

4. The coupled finite-element method

As shown in figure 2, the coupled finite-element method divides the fluid domain into a region R_1 surrounding the cylinder and a region R_2 tending to infinity. We impose the Laplace equation in a uniform sense in region R_1, or

$$\iint_{R_1} \nabla^2\phi\psi \,\mathrm{d}x\,\mathrm{d}z = 0, \tag{21}$$

where ψ is an appropriately chosen weight function. Using Green's identity, we obtain

$$\iint_{R_1} \nabla\phi\cdot\nabla\psi \,\mathrm{d}x\,\mathrm{d}z - \int_{S_J} \frac{\partial\phi}{\partial n}\phi \,\mathrm{d}S = \int_{S_0} \frac{\partial\phi}{\partial n}\psi \,\mathrm{d}S, \tag{22}$$

where S_J is the outer boundary of R_1 (or the inner boundary of R_2) and is assumed fully submerged in the present problem of a submerged body. In (22), $\partial\phi/\partial n$ on the right-hand side is known from the body surface condition; and $\partial\phi/\partial n$ on the left-hand side can be determined from the following boundary integral equation over S_J:

$$\phi(P) = \frac{1}{\alpha}\int_{S_J}\left[G(P,Q)\frac{\partial\phi(Q)}{\partial n} - \frac{\partial G(P,Q)}{\partial n}\phi(Q)\right]\mathrm{d}S \tag{23}$$

obtained from the second Green's identity in the outer domain R_2, where α is the subtended exterior angle at point P and the direction of $\boldsymbol{n}$ is from R_1 to R_2. By discretization of this equation using the finite-element shape function, we can express $\partial\phi/\partial n$ as a function of ϕ on S_J. By substitution of the result into (22) a governing equation for potentials on the nodes of the finite elements can be obtained. The detailed numerical process for obtaining the results below follows that in the work on infinite water depth (Wu & Eatock Taylor 1987).

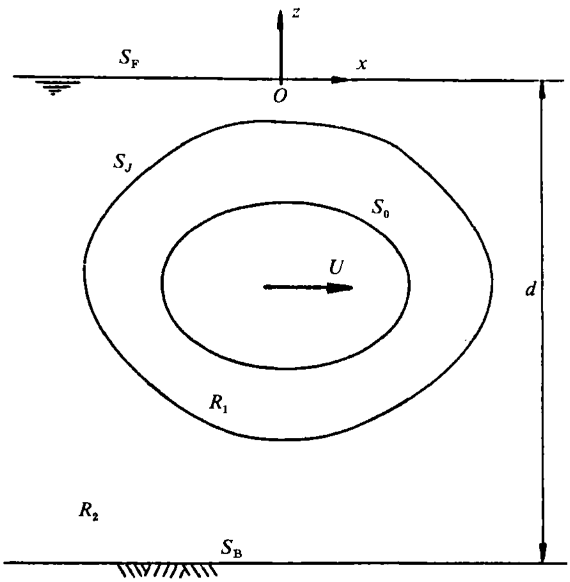

FIGURE 2. Definition of geometry and fluid regions.

5. Hydrodynamic coefficients

The steady potential $\bar{\phi}$ and the related wave resistance on a submerged cylinder have been obtained by Eatock Taylor & Wu (1986) using the coupled finite-element method. The solution is employed here in the body-surface boundary condition in (11a) on the radiation potentials. Thus we only give a discussion on the unsteady potential. However, as the solution of the steady potential of a floating cylinder is not unique (Ursell 1980), the discussion is limited to a submerged cylinder.

After the velocity potential is found, the added masses μ_{ij} and damping coefficients λ_{ij} can be obtained from (Newman 1978)

$$\tau_{ij} = \omega^2 \mu_{ij} - \mathrm{i}\omega\lambda_{ij} = -\rho \int_{S_0} (\mathrm{i}\omega\phi_j + \boldsymbol{W}\cdot\nabla\phi_j)\, n_i \,\mathrm{d}S, \tag{24}$$

where ρ is the density of the fluid and

$$\boldsymbol{W} = U\nabla(\bar{\phi} - x). \tag{25}$$

Equation (24) may also be written in the following form (Wu & Eatock Taylor 1988b):

$$\tau_{ij} = \rho \int_{S_0} \frac{\partial \phi_i^*}{\partial n}\phi_j \,\mathrm{d}S, \tag{26}$$

where the symbol * denotes the complex conjugate. Thus

$$\tau_{ij} - \tau_{ji}^* = \rho \int_{S_0} \left[\frac{\partial \phi_i^*}{\partial n}\phi_j - \frac{\partial \phi_j}{\partial n}\phi_i^*\right] \mathrm{d}S$$
$$= -\rho \int_{S_F + S_\infty} \left[\frac{\partial \phi_i^*}{\partial n}\phi_j - \frac{\partial \phi_j}{\partial n}\phi_i^*\right] \mathrm{d}S,$$

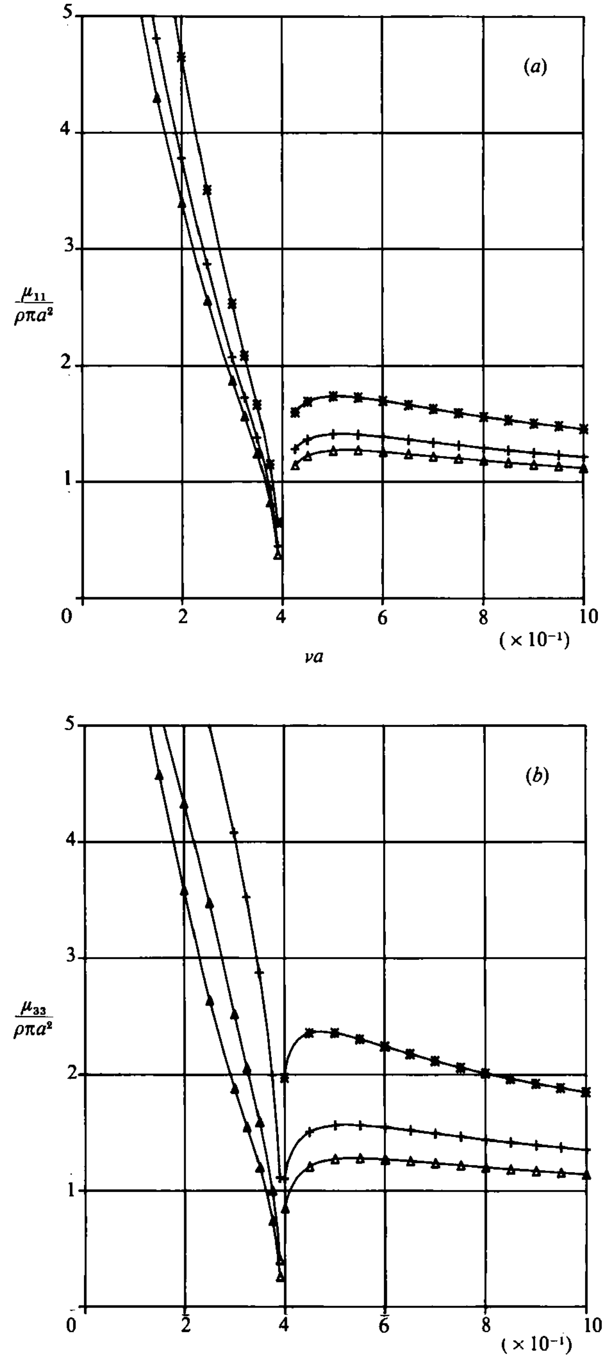

FIGURE 3. The added masses of a circular cylinder in water of different depths ($h = 2a, Fn = 0.4$); (a) surge, (b) heave. —△—, $d = 10a$, $\nu_c a = 0.3906$; —+—, $d = 4.5a$, $\nu_c a = 0.3906$; —*—, $d = 3.5a$, $\nu_c a = 0.3906$.

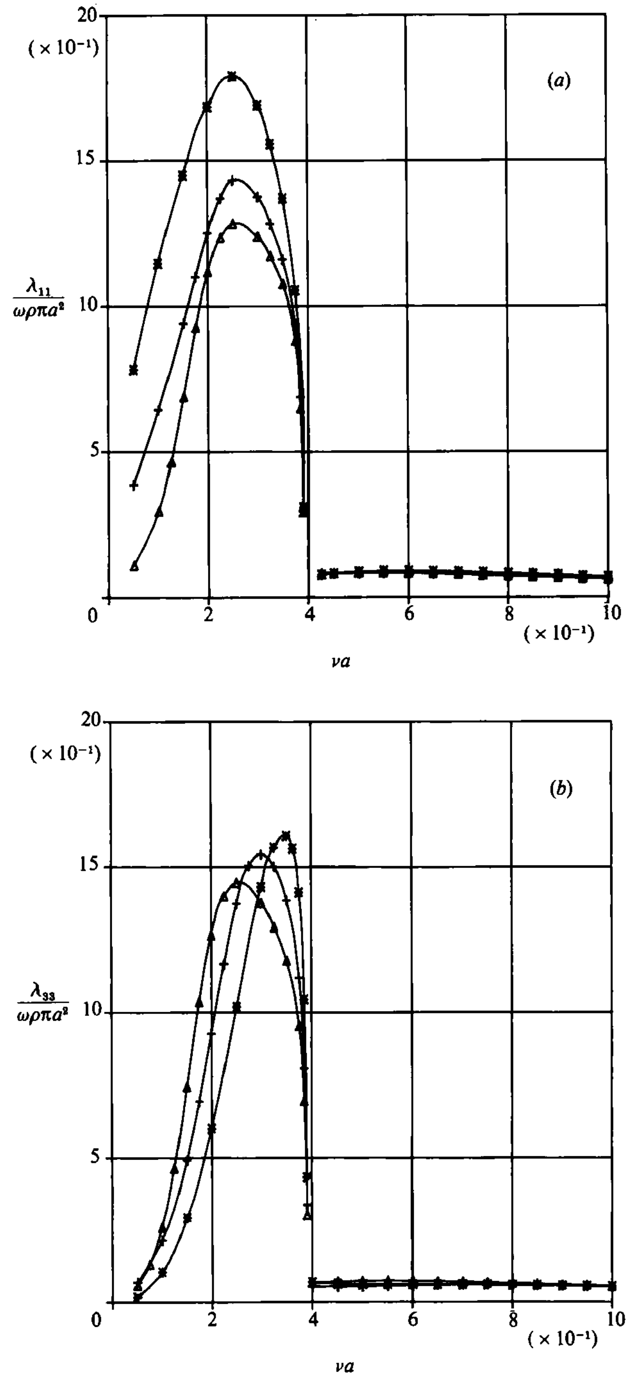

FIGURE 4. The damping coefficients of a circular cylinder in water of different depths ($h = 2a, Fn = 0.4$); (*a*) surge, (*b*) heave. Symbols as figure 3.

where S_∞ is the surface at infinity and may be taken as two vertical lines at $x \to \pm\infty$. Invoking the free-surface boundary condition on ϕ, we obtain

$$\tau_{ij} - \tau_{ji}^* = \rho\left[\frac{\tau^2}{\nu}(\phi_{ix}^*\phi_j - \phi_{jx}\phi_i^*) + 2\mathrm{i}\tau\phi_i^*\phi_j\right\}_{-\infty}^{+\infty} - \rho\int_{S_\infty}(\phi_{in}^*\phi_j - \phi_{jn}\phi_i^*)\,\mathrm{d}S.$$

Since $\qquad \phi_j \to A_{2j}\cosh k_2(z+d)\,\mathrm{e}^{-\mathrm{i}k_2 x}/\cosh k_2 d \quad \text{as} \quad x \to +\infty,$

where i in A_{ij} corresponds to that in k_i, and j indicates jth mode of the motions, we can obtain the contribution from the k_2 wave to the above equation as

$$I_2 = \frac{\tau^2}{\nu}2\mathrm{i}k_2 A_{2i}^* A_{2j} + 2\mathrm{i}\tau A_{2i}^* A_{2j} - 2\mathrm{i}k_2\left[\tfrac{1}{2}d + \frac{1}{4k_2}\sinh(2k_2 d)\right]\operatorname{sech}^2(k_2 d)A_{2i}^* A_{2j}.$$

From the governing equation for k_2, this equation becomes

$$I_2 = \mathrm{i}A_{2i}^* A_{2j}\left[\frac{\tau^2}{\nu}k_2 - \frac{\nu}{k_2} - k_2 d\operatorname{sech}^2(k_2 d)\right].$$

Using

$$\phi_j \to \frac{A_{1j}\cosh k_1(z+d)\,\mathrm{e}^{-\mathrm{i}k_1 x}}{\cosh k_1 d} + \frac{A_{3j}\cosh k_3(z+d)\,\mathrm{e}^{\mathrm{i}k_3 x}}{\cosh k_3 d} + \frac{A_{4j}\cosh k_4(z+d)\,\mathrm{e}^{\mathrm{i}k_4 x}}{\cosh k_4 d} \quad \text{as} \quad x \to -\infty$$

we can obtain the similar contributions from k_1, k_3 and k_4 and the final result can be written as

$$\begin{aligned}\tau_{ij} - \tau_{ji}^* = \rho\mathrm{i}\Big\{ & -A_{1i}^* A_{1j}\left[\frac{\tau^2}{\nu}k_1 - \frac{\nu}{k_1} - k_1 d\operatorname{sech}^2(k_1 d)\right] \\ & + A_{2i}^* A_{2j}\left[\frac{\tau^2}{\nu}k_2 - \frac{\nu}{k_2} - k_2 d\operatorname{sech}^2(k_2 d)\right] \\ & + A_{3i}^* A_{3j}\left[\frac{\tau^2}{\nu}k_3 - \frac{\nu}{k_3} - k_3 d\operatorname{sech}^2(k_3 d)\right] \\ & + A_{4i}^* A_{4j}\left[\frac{\tau^2}{\nu}k_4 - \frac{\nu}{k_4} - k_4 d\operatorname{sech}^2(k_4 d)\right]\Big\}. \qquad (27)\end{aligned}$$

Unlike the case of zero forward speed, no relation such as $\tau_{ij} = \tau_{ji}$ (e.g. Mei 1982) is found in general. Thus (27) does not provide a means for calculating the individual hydrodynamic coefficients. However, the special case $i = j$ reduces (27) to

$$\begin{aligned}\lambda_{jj} = \frac{-\rho}{2\omega}\Big\{ & -|A_{1j}|^2\left[\frac{\tau^2}{\nu}k_1 - \frac{\nu}{k_1} - k_1 d\operatorname{sech}^2(k_1 d)\right] \\ & + |A_{2j}|^2\left[\frac{\tau^2}{\nu}k_2 - \frac{\nu}{k_2} - k_2 d\operatorname{sech}^2(k_2 d)\right] \\ & + |A_{3j}|^2\left[\frac{\tau^2}{\nu}k_3 - \frac{\nu}{k_3} - k_3 d\operatorname{sech}^2(k_3 d)\right] \\ & + |A_{4j}|^2\left[\frac{\tau^2}{\nu}k_4 - \frac{\nu}{k_4} - k_4 d\operatorname{sech}^2(k_4 d)\right]\Big\}. \qquad (28)\end{aligned}$$

This enables us to calculate the hydrodynamic damping from an alternative equation to (24). As $d \to \infty$, (28) can be found to be virtually identical to that in infinite water depth derived by Grue & Palm (1985) from energy conservation (noting they have used the wave amplitude in the equation). For supercritical flow the terms involving k_1 and k_2 should be deleted from (28).

Another special case of (27) is when forward speed is very large. As $U \to \infty$ the solutions k_1 and k_2 do not exist and $k_3 = k_4 \to \omega/U$. This gives

$$\tau_{ij} - \tau_{ji}^* = 0, \tag{29}$$

which has been proved by Wu & Eatock Taylor (1988*a*) for the general case of the linearized potential theory.

Figures 3 and 4 give the hydrodynamic coefficients for a circular cylinder submerged at $h = 2a$ in fluid of different depths (a is the radius of the cylinder and h is the distance from the centre of the cylinder to the free surface), using a mesh of 12 elements which provides sufficient accuracy. The results are plotted against νa at the Froude number $Fn = U/(ga)^{\frac{1}{2}} = 0.4$. ν_c is defined as the critical point at which both (18) and (19) are satisfied. Since the added mass and damping coefficient associated with the rotation of a circular cylinder about its centre are zero, they are omitted from the figures. Equation (28) is used to check the damping coefficients λ_{jj} obtained from (24) and excellent agreement is found. Since it is also observed that the equation $\tau_{31} = -\tau_{13}$ for a symmetrical cylinder (Timman & Newman 1962; Newman 1965; Wu & Eatock Taylor 1990) is satisfied at this Froude number, results for τ_{13} are omitted.

From the calculation, we found that the effect of the water depth becomes significant when $d < 10a$ for the case in figures 3 and 4. However, in the calculated region $3.5a < d < 10a$, the water depth does not affect the first four figures of the critical point. This is mainly because $Fn = 0.4$ corresponds to a low speed. The results change sharply near ν_c, but they do not suggest discontinuity (Mo & Palm 1987).

6. The exciting forces and moments

We now consider the diffraction problem. The incident potential may be written as

$$\phi_0 = -\frac{ig}{\omega_0}\frac{\cosh k_0(z+d)}{\cosh k_0 d}\,\mathrm{e}^{\pm \mathrm{i}k_0 x}, \tag{30}$$

where + and − signs correspond to a wave from the right and left respectively. After the diffraction ϕ_7 is found, the exciting force and moment can be obtained from (Newman 1978)

$$F_j = -\rho\eta_0 \int_{S_0} [\mathrm{i}\omega(\phi_0+\phi_7) + \boldsymbol{W}\cdot\nabla(\phi_0+\phi_7)]\, n_j\,\mathrm{d}S. \tag{31a}$$

Similar to (24), equation (31*a*) may be written as

$$F_j = \rho\eta_0 \int_{S_0} \frac{\partial \phi_j^*}{\partial n}(\phi_0+\phi_7)\,\mathrm{d}S. \tag{31b}$$

Since the diffraction potential satisfies the same free-surface and radiation conditions as the radiation potential, an equation similar to (27) containing the amplitudes of the diffraction potential can be easily obtained. However, care is needed for the incident potential since it does not satisfy the radiation condition. We first consider

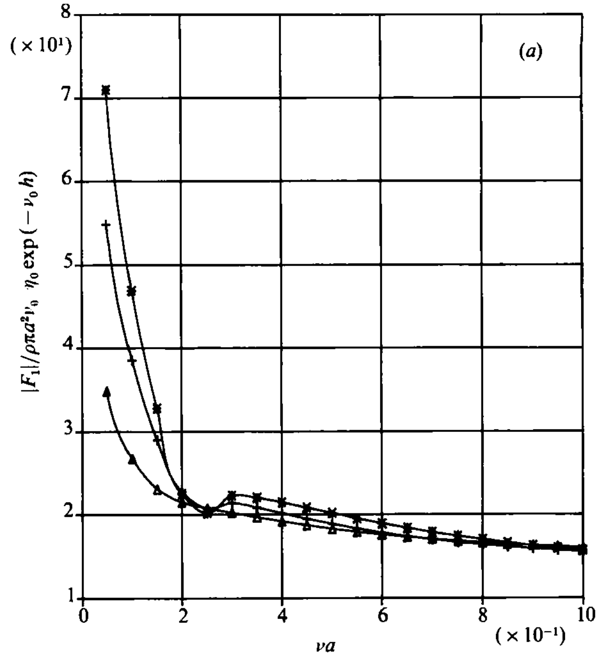

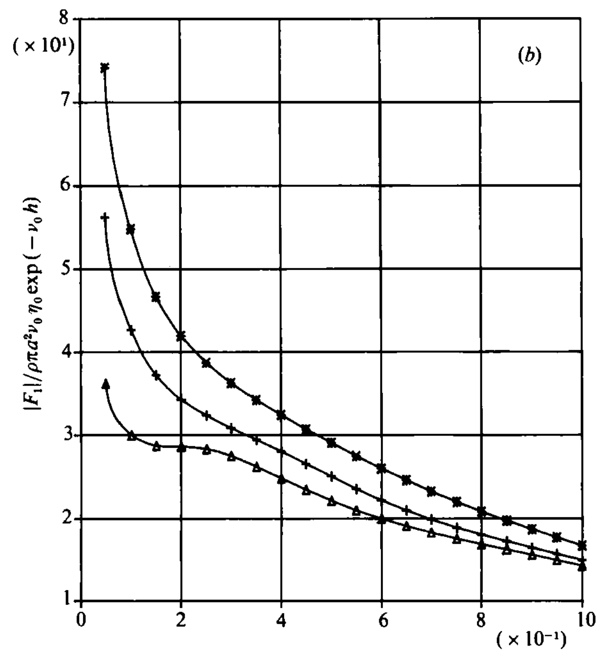

FIGURE 5. The amplitude of the surge exciting force on a circular cylinder in water of different depths ($h = 2a, Fn = 0.4$); (a) wave from the right, —△—, $d = 10a, \nu_{0c}a = 2678$; —+—, $d = 4.5a, \nu_{0c}a = 0.2568$; —∗—, $d = 3.5a, \nu_{0c}a = 0.2498$. ($b$) Wave from the left, —△—, $d = 10a$, $\nu_{0c}a = 0.3906,\ 9.1069$; —+—, $d = 45a, \nu_{0c}a = 0.3906,\ 9.1609$; —∗—, $d = 3.5a, \nu_{0c}a = 0.3906$, 9.1068.

the case of a wave from the right. It can easily be found that k_0 is identical to k_4. This immediately gives

$$F_j = \rho i \eta_0 \left\{ -A^*_{1j} A_{17} \left[\frac{\tau^2}{\nu} k_1 - \frac{\nu}{k_1} - k_1 d \operatorname{sech}^2(k_1 d) \right] \right.$$
$$+ A^*_{2j} A_{27} \left[\frac{\tau^2}{\nu} k_2 - \frac{\nu}{k_2} - k_2 d \operatorname{sech}^2(k_2 d) \right]$$
$$- A^*_{3j} A_{37} \left[\frac{\tau^2}{\nu} k_3 - \frac{\nu}{k_3} - k_3 d \operatorname{sech}^2(k_3 d) \right]$$
$$\left. - A^*_{4j} \left(A_{47} - \frac{ig}{\omega_0} \right) \left[\frac{\tau^2}{\nu} k_4 - \frac{\nu}{k_4} - k_4 d \operatorname{sech}^2(k_4 d) \right] \right\}. \tag{32a}$$

When there is no solution from (18), the terms involving k_1 and k_2 in the above equation should be deleted.

When the wave is from the left, we have $k_0 = k_2$ if the group velocity of the incoming wave $C_{g0} > U$, and $k_0 = k_1$ if $C_{g0} < U$. In the first case, we have

$$F_j = \rho i \eta_0 \left\{ -A^*_{1j} A_{17} \left[\frac{\tau^2}{\nu} k_1 - \frac{\nu}{k_1} - k_1 d \operatorname{sech}^2(k_1 d) \right] \right.$$
$$+ A^*_{2j} \left(A_{27} - \frac{ig}{\omega_0} \right) \left[\frac{\tau^2}{\nu} k_2 - \frac{\nu}{k_2} - k_2 d \operatorname{sech}^2(k_2 d) \right]$$
$$- A^*_{3j} A_{37} \left[\frac{\tau^2}{\nu} k_3 - \frac{\nu}{k_3} - k_3 d \operatorname{sech}^2(k_3 d) \right]$$
$$\left. - A^*_{4j} A_{47} \left[\frac{\tau^2}{\nu} k_4 - \frac{\nu}{k_4} - k_4 d \operatorname{sech}^2(k_4 d) \right] \right\}, \tag{32b}$$

while in the second case the term $-ig/\omega_0$ should be included in A_{17}. Complexity arises when $U > \omega_0/k_0$, since the encounter frequency becomes negative. As a negative encounter frequency has no apparent physical meaning, the time factor in (1) should be taken as $e^{-i\omega t}$, while

$$\omega = k_0 U - \omega_0. \tag{33}$$

The sign of the first term on the right-hand side of (11 a) should be correspondingly changed and the Green function employed in (23) should be replaced by G^*. The physical interpretation of $U > \omega_0/k_0$ is that the cylinder overtakes the incident wave. In the coordinate system moving with the cylinder one actually sees that the wave is from the right. It gives $k_0 = k_3$ and the term $-ig/\omega$ should be included in A_{37}. Finally, analogous to the case of a wave from the right, when there is no solution from (18), the terms involving k_1 and k_2 should be deleted from (32 b).

Figures 5 (a) and 5 (b) give the surge exciting forces on the circular cylinder considered in figures 3 and 4, and corresponding to the incoming wave from the right and left respectively, while figures 6 (a) and 6 (b) give the heave forces. The results are now plotted against $\nu_0 a (\nu_0 = \omega_0^2/g)$ and are non-dimensionalized by $\rho g \pi a^2 (\nu_0 \eta_0 e^{-\nu_0 h})$. The problem here is quite different from that without forward speed. The figures show that even for a symmetric cylinder, incoming waves from the right and left give different results. This is mainly because they lead to different encounter frequencies as shown by (2 a). When the wave is from the left, there will be two critical points,

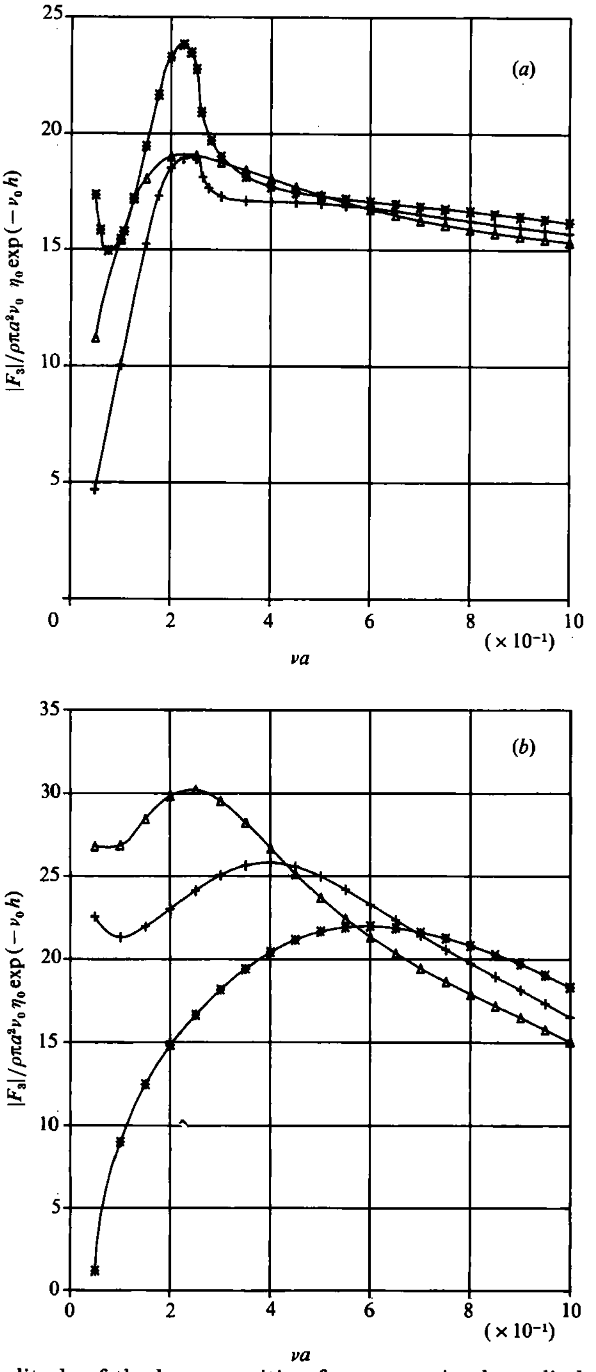

FIGURE 6. The amplitude of the heave exciting force on a circular cylinder in water of different depths ($h = 2a, Fn = 0.4$); (*a*) wave from the right, (*b*) wave from the left. Symbols as figure 5.

one of which corresponds to $\omega > 0$ and the other to $\omega < 0$. For both incoming wave directions, the effect of water on the exciting forces is mainly in the low-frequency or short-wavelength range.

Figures 7 and 8 give the results for an elliptical cylinder with an upward attack

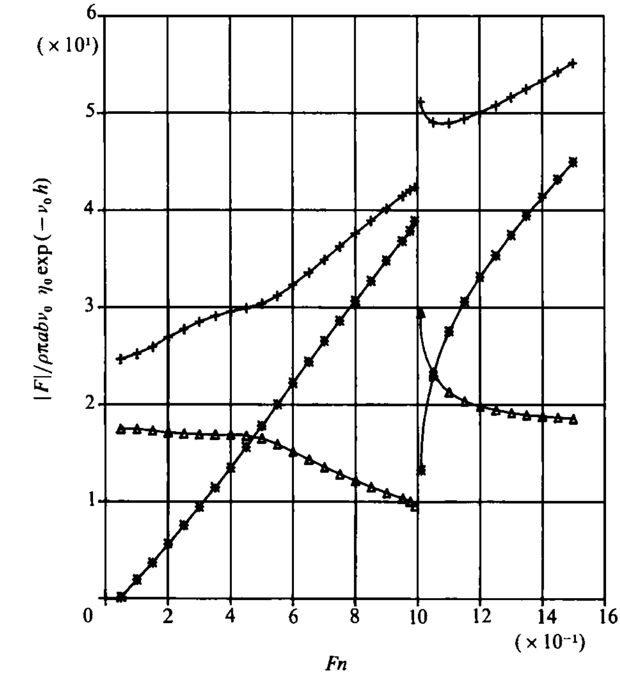

FIGURE 7. The influence of forward speed on the exciting force and moment on an elliptic cylinder ($h = 2a$, $a = 2b$, $d = 3.5a$, $\nu_0 a = 0.5$, $Fn_c = 0.1554$), wave from the right. —△—, $|F_1|$; —+—, $|F_3|$; —∗—, $|F_5|$.

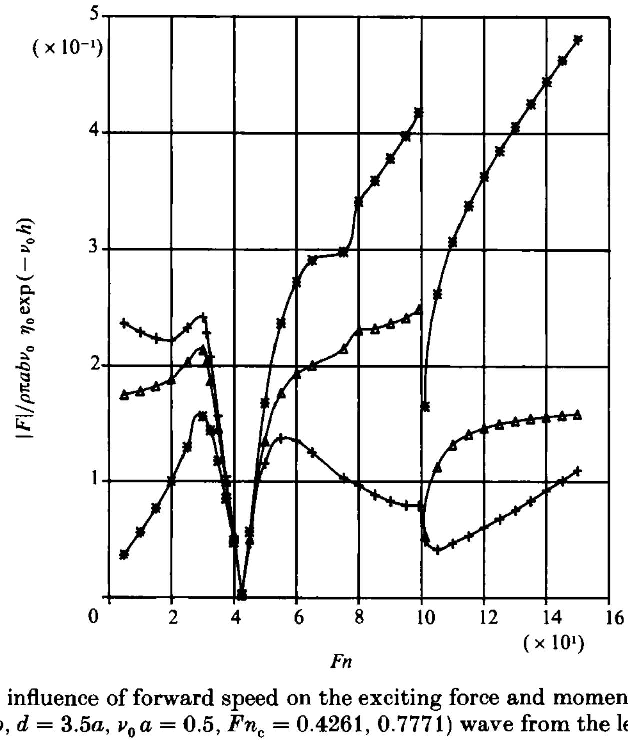

FIGURE 8. The influence of forward speed on the exciting force and moment on an elliptic cylinder ($h = 2a$, $a = 2b$, $d = 3.5a$, $\nu_0 a = 0.5$, $Fn_c = 0.4261$, 0.7771) wave from the left. Symbols as figure 7.

angle of 10° and submerged at $h = 2a$ with $a = 2b$ (a is the major axis and b minor axis). Following the increase of the Froude number $Fn = U/(gh)^{\frac{1}{2}}$ we have $k_2 = k_0$ at low speed. As the forward speed increases, it reaches the critical point at $Fn = 0.4261$ corresponding to $U = C_{g0}$. As the cylinder advances at the same speed as the wave group velocity at this point, the exciting forces approach zero. Unlike the radiation problem of the forced oscillatory motion, the flow does not become supercritical after the critical point. Instead, the flow returns to subcritical but with $k_1 = k_0$. This can be understood from (2a) and figure 1 which show that for a given wave frequency the encounter frequency ω decreases as U increases. As the forward speed further increases, the encounter frequency becomes zero at $Fn = 0.7188$ and correspondingly $U = \omega_0/k_0$. The wave is stationary in the moving coordinate system at this particular point. After that the wave will be from the right in the moving system. It later reaches its other critical point at $Fn = 0.7771$ corresponding to $U = C_{g0}$ and $k_1 = k_2$. Only after that does the oscillatory flow become supercritical. As the forward speed further increases to $Fn = 1.0$, the steady flow will become supercritical and this leads to discontinuity of the exciting forces.

The financial support by Cray Research (UK) Ltd is acknowledged.

REFERENCES

Becker, V. E. 1956 Die pulsierende Quelle unter der freien Oberflache eines Stromes endlicher Tiefe. *Ing.-Arch.* **24**, 69–76.

Eatock Taylor, R. & Wu, G. X. 1986 Wave resistance and lift on cylinders by a coupled element technique. *Intl Shipbuilding Prog.* **33**, 2–9.

Grue, J. & Palm, E. 1985 Wave radiation and wave diffraction from a submerged body in a uniform current. *J. Fluid Mech.* **151**, 257–278.

Mei, C. C. 1982 *The Applied Dynamics of Ocean Waves.* Wiley-Interscience.

Mo, O. & Palm, E. 1987 On radiated and scattered waves from a submerged elliptical cylinder in a uniform current. *J. Ship Res.* **31**, 23–33.

Newman, J. N. 1961 The exciting forces on a moving body in waves. *J. Ship Res.* **9**, 190–199.

Newman, J. N. 1978 The theory of ship motions. *Adv. Appl. Mech.* **18**, 221–283.

Timman, R. & Newman, J. N. 1962 The coupled damping coefficients of a symmetric ship. *J. Ship Res.* **5**, 1–7.

Ursell, F. 1980 Mathematical notes on the two-dimensional Kelvin–Neumann problem. In *13th Symp. on Naval Hydrodyn.*, vol. 2.

Wu, G. X. & Eatock Taylor, R. 1987 Hydrodynamic forces on submerged oscillating cylinders at forward speed. *Proc. R. Soc. Lond.* A **414**, 149–170.

Wu, G. X. & Eatock Taylor, R. 1988*a* Reciprocity relations for hydrodynamic coefficients of bodies with forward speed. *Intl Shipbuilding Prog.* **35**, 145–153.

Wu, G. X. & Eatock Taylor, R. 1988*b* Radiation and diffraction of water waves by a submerged sphere at forward speed. *Proc. R. Soc. Lond.* A **417**, 433–461.

Wu, G. X. & Eatock Taylor, R. 1990 The hydrodynamic force on an oscillating ship with low forward speed. *J. Fluid Mech.* **211**, 333–353.